ELSEVIER

Inorganica Chimica Acta 225 (1994) 23–34

Inorganica Chimica Acta

Charge and electron transfer from metal-to-carbon bonds of main group organometallics MR_n (M = Al, Ga, Zn) to aromatic N-heterocycles: colored precursor compounds and radical complex formation

Steffen Hasenzahl, Wolfgang Kaim*, Thomas Stahl

Institut für Anorganische Chemie der Universität, Pfaffenwaldring 55, D-70550 Stuttgart, Germany

Received 10 February 1994

Abstract

The coordinatively unsaturated compounds AlR_3, GaR_3 and ZnR_2, R = isopropyl, were reacted with linearly bridging pyrazine, tetramethylpyrazine or 4,4′-bipyridine ligands and with potentially chelating 2,2′-bipyridine. The primary reaction products are diamagnetic dinuclear complexes ('bis-adducts') which are characterized by intense long-wavelength ligand-to-ligand charge transfer (LLCT) transitions $\sigma(M\text{–}R) \rightarrow \pi^*(L)$ and which may yield radical complexes after loss of R·. The latter reaction is assumed to have a strong single electron transfer (SET) component. An isolable 'Al(II)' species (bpy)Al$[CH(SiMe_3)_2]_2$ has been characterized unambiguously by ESR, UV–Vis and cyclic voltammetry as an Al(III) complex of the bpy radical anion. Irradiation into the fairly intense LLCT absorption bands ($\epsilon > 3000\ M^{-1}\ cm^{-1}$) of the dinuclear complexes between pyrazine and Al^iPr_3 or Ga^iPr_3 resulted in bleaching and formation of a mixture of non-aromatic products. Attempts are made to correlate charge transfer properties and radical formation with the geometrical and electronic structures of the precursor complexes.

Keywords: Charge transfer; Electron transfer; Metal complexes; Aromatic heterocycle complexes; Main group elements

1. Introduction

In contrast to classical or organometallic compounds of the transition elements, the organic derivatives of the main group metals have received relatively little attention with respect to their electron transfer chemistry, especially with regard to the photoinduced variety [1–3]. On the other hand, these substances certainly enjoy a quantitatively wider distribution than the transition metal analogues due to their in-bulk availability and due to their long recognized usefulness in polymer chemistry and organic synthesis [4,5].

For instance, group transfer reactions, formulated via a concerted way in (1) can be formally separated into elementary steps including single electron transfer (SET) processes (2) [6]. While transition metal chemistry has no problems with SET mechanistic concepts because odd-electron oxidation states with incompletely filled d orbitals are well established [7,8], the apparent SET reactivity of main group metal compounds, e.g. of low-valent indium or tin compounds with suitable acceptor substrates [9], is being viewed as unusual. SET reactivity of main group metals in their 'normal' oxidation states with noble gas electron configuration requires an active ligand such as a 'carbanion' in corresponding organometallic compounds. In fact, there is now an increasing number of reactions between organic compounds and organometallic derivatives of the main group elements which seem to involve single electron transfer steps, i.e. the splitting of electron pairs [11]. The identification of SET processes has sometimes been controversial due to the mechanistic alternative [10] between a 'normal' (i.e. concerted) but polar S_N2 reaction and a SET process (2), however, the concept of a tight inner-sphere electron transfer situation may attenuate this apparent dichotomy [11].

*Corresponding author.

SSDI 0020-1693(94)04025-Q

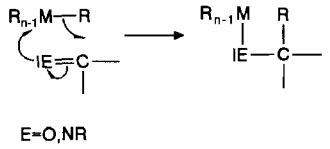

(1)

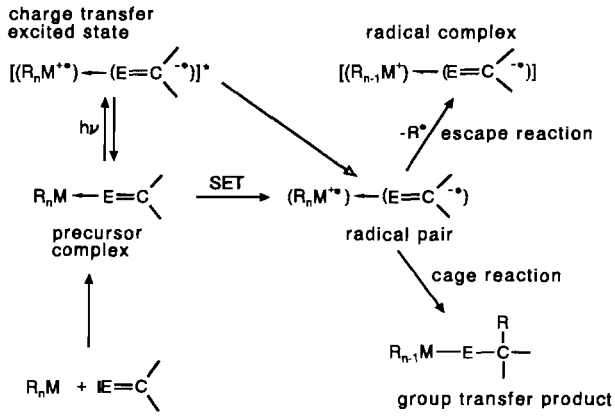

(2)

In spite of the mechanistic uncertainty, the undisputed polarity of the metal-to-carbon bond, i.e. the considerably unsymmetrical electron distribution $M^{\delta+}$–$C^{\delta-}$, invites an interaction with typical acceptor substrates which are capable of removing one or two electrons from the metal-to-carbon σ bond, thus contributing to its cleavage (3) [1,2].

$$R_{n-1}M\text{–}R \xrightarrow{-e^-} [R_{n-1}M\cdot R]^+ \longrightarrow R_{n-1}M^+ + R^\cdot \quad (3)$$

Electrochemistry as an obvious technique to study electron transfer processes [12,13] is often experimentally and conceptually difficult in the case of the oxidation of simple main group organometallics [1,2]; the reactions are generally irreversible, produce strongly adsorbing intermediates, and may not even be attributable to defined species because of the well-known solvation, aggregation, ligand exchange and autoionization equilibria (4) of coordinatively unsaturated main group organometallics [4,5]. The latter phenomena are all due to the simultaneous presence of a coordinatively unsaturated electrophilic metal center *and* of electron-rich 'carbanionic' substituents, implicating high lying molecular orbitals σ(M–C).

$$2R_nM \rightleftharpoons R_{n+1}M^- + R_{n-1}M^+ \text{ (solv.)} \quad (4)$$

A way out of this dilemma is to use thermally stable precursor complexes (2) [12] between the acceptor substrate and the organometallic donor which then contain coordinatively saturated metal centers. Such persistent precursor complexes of potential inner-sphere electron transfer reactions may be found particularly among the Group 12 and 13 organometallic compounds which are still coordinatively unsaturated (unlike most Group 14 organometallics) but which are not too electropositive and thus thermally not too reactive, as would be typical for organometallics of Group 1 and 2 elements [1]. Typically, such precursor complexes between σ accepting (i.e. Lewis acidic) and σ(M–C) electron-donating organometallics on one side and σ donating (i.e. Lewis basic) and π electron-accepting acceptor ligands on the other side show long-wavelength absorptions which may be attributed to potentially photoreactive ligand-to-ligand charge transfer (LLCT [14]) transitions $\sigma(M\text{–}C) \rightarrow \pi^*$ (5) [1,6].

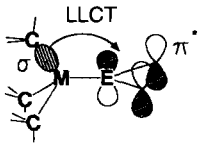

(5)

In this paper we describe the results obtained in reacting trialkylaluminium(III), trialkylgallium(III) and dialkylzinc(II) compounds with the unsaturated N-heterocycles pyrazine (pz), 2,3,5,6-tetramethylpyrazine (tmpz), 4,4′-bipyridine (bp) and 2,2′-bipyridine (bpy) (6). While the first three acceptors are able to act as linearly bridging ligands, bpy usually prefers a chelate coordination, although it can also serve as non-chelating ligand [15–17]. Different steric situations (pz versus tmpz) and different π acceptor behavior may be assumed for the three linearly bridging ligands. As alkyl substituents at the main group metals we used electron-rich and fairly bulky isopropyl and bis(trimethylsilyl)-methyl groups. These groups were chosen because of their electron-donating characteristics [18] and because their size promised to impede aggregation, stabilize precursors and intermediates [19], and allow electrochemical experiments without electrode deactivation [12].

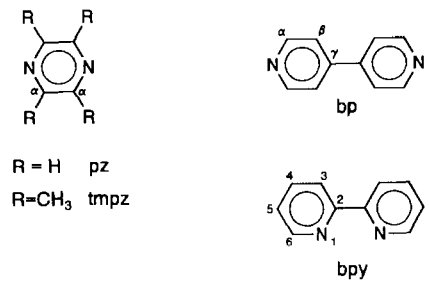

(6)

2. Results and discussion

2.1. Dinuclear complexes of bridging ligands

All diamagnetic precursor complexes are colored but highly air- and moisture-sensitive and dissociable compounds which could only be crystallized from non-coordinating solvents. They were, however, unambiguously characterized by ^1H and ^{13}C NMR and by absorption spectroscopy in such solvents.

2.1.1. Complexes $(\mu\text{-L})(AlR_3)_2$

2.1.1.1. Synthesis and stability

The very air-sensitive dark red compound $(pz)(Al^iPr_3)_2$ had been described before [20]. The even more sensitive red crystals of $(tmpz)(Al^iPr_3)_2$ slowly disintegrated at ambient temperatures and had to be stored at −30 °C. The orange complex $(bp)(Al^iPr_3)_2$ was less sensitive than the pyrazine complexes. Attempts to prepare $(pz)\{Al[CH(SiMe_3)_2]_3\}_2$ from the components failed, presumably because steric hindrance precludes the necessary pyramidalization at Al. Steric and electronic effects of the bridging ligands can be correlated straightforwardly with the above mentioned stability of the complexes. Compared to pyrazine (pK_a 0.65 [21a], 4,4′-bipyridine is a much stronger base (pK_a 4.82 [21b]) with better metal σ bonding; on the other hand, coordination to the nitrogen centers of tetramethylpyrazine is impaired by repulsive interactions with the methyl groups [22].

2.1.1.2. NMR spectroscopy

The charge transfer character of the dinuclear triorganoaluminium complexes is evident not only from the color (see below) but also from the ^1H NMR data obtained in C_6D_6 (Tables 1 and 2). In general, the nuclei of the isopropyl substituents experience a low-field shift whereas the protons of the heterocyclic acceptors are shifted to higher field upon coordination. For the ^{13}C NMR data, the situation is more complex, reflecting π electron redistribution.

2.1.1.3. Electrochemistry

Cyclic voltammetric studies could be carried out in chlorinated hydrocarbon electrolyte solutions for the pz [20] and bp complexes; the tmpz complex proved to be too labile for such measurements. The results (Table 3) show irreversible oxidation at rather low potentials, corresponding to electron removal from the 'carbanion' substituents [2,20], and reversible reduction to radical anion complexes $(\mu\text{-L}^{\cdot-})(AlR_3)_2$ [3,23]. The much facilitated reduction of both complexes in comparison to the free ligands is a consequence [24] of the strong Lewis acidity (σ acceptor capability) of two coordinated triorganoaluminium molecules; in agreement with established MO concepts [25], the smaller π system pz with its higher π^* MO coefficient at the nitrogen centers exhibits a stronger effect than the larger π system of bp. As a consequence, the pz complex is easier reduced than the bp analogue although the reverse holds for the free ligands.

Table 1
^1H chemical shifts δ (ppm) of the complexes $(\mu\text{-L})(MR_n)_2$, R = ^{i}Pr, and the free components[a]

	Isopropyl group[b]		Heterocycle		
	$CH(CH_3)_2$	$CH(CH_3)_2$	CH_3	α-H	β-H
pz				8.07	
tmpz			2.23		
bp				6.84[c]	8.56[c]
AlR_3	0.36	1.14			
$(pz)(AlR_3)_2$	0.51	1.26		7.79	
$(tmpz)(AlR_3)_2$	0.62	1.27	2.12		
$(bp)(AlR_3)_2$	0.79	1.51		6.44[c]	8.22[c]
GaR_3	0.98	1.21			
$(pz)(GaR_3)_2$	1.02	1.31		7.77	
$(bp)(GaR_3)_2$	1.26	1.55		6.65[c]	8.39[c]
ZnR_2	0.59	1.19			
$(pz)(ZnR_2)_2$	0.74	1.25		7.96	
$(tmpz)(ZnR_2)_2$	0.73	1.32	2.08		

[a]In C_6D_6.
[b]Septet and doublet, ^3J = 7.1–7.8 Hz.
[c]Doublet, ^3J = 6.1–6.6 Hz.

Table 2
^{13}C chemical shifts δ (ppm) of the complexes $(\mu\text{-L})(MR_n)_2$, R = ^{i}Pr, and the free components[a]

	Isopropyl group		Heterocycle			
	$CH(CH_3)_2$	$CH(CH_3)_2$	CH_3	α-C	β-C	γ-C
pz				145.2		
tmpz			21.2	148.2		
bp				151.0	121.2	145.1
AlR_3	11.9	20.0				
$(pz)(AlR_3)_2$	8.9	21.1		144.0		
$(tmpz)(AlR_3)_2$	12.2	21.1	21.3	151.1		
$(bp)(AlR_3)_2$	9.3	21.6		148.4	122.6	146.5
GaR_3	19.9	20.7				
$(pz)(GaR_3)_2$	14.0	22.0		144.4		
$(bp)(GaR_3)_2$	13.6	22.5		150.0	121.6	[b]
ZnR_2	18.8	21.5				
$(tmpz)(ZnR_2)_2$	17.7	20.5	22.8	148.5		

[a]In C_6D_6.
[b]Not detected.

Table 3
Electrochemical potentials of the complexes $(\mu\text{-L})(MR_3)_2$, R = ^{i}Pr, and the free ligands in dichloroethane/0.1 M Bu_4NPF_6[a]

	$E_{1/2}$(red)	E_{pa}(ox)	ΔE_{pa}[d]
bp	−1.80		
pz	−2.10		
$(pz)(AlR_3)_2$	−0.77[c]	0.85	1.50
$(bp)(AlR_3)_2$	−1.08[c]	0.81	1.78
$(pz)(GaR_3)_2$[b]	−1.27[c]	0.71	1.92

[a]From cyclic voltammetry at 100 mV/s; potentials in V vs. SCE.
[b]In CH_2Cl_2/0.1 M Bu_4NPF_6.
[c]Quasi-reversible waves (ΔE_{pp} = 0.1–0.2 V).
[d]Difference of anodic peak potentials for oxidation and reduction.

2.1.1.4. Absorption spectroscopy

The absorption spectra of all three complexes in pentane show intense, broad long-wavelength bands (Table 4) which are attributed to LLCT transitions. This interpretation $\sigma(M\text{–}R) \rightarrow \pi^*(L)$ (5) [1,6] is in agreement with the results from cyclic voltammetry,

Table 4
Absorption maxima of the complexes $(\mu\text{-L})(MR_n)_2$, R = ^{i}Pr, in aliphatic hydrocarbons[a]

	λ_{max} (nm) (ϵ (M^{-1} cm^{-1}))	$\tilde{\nu}_{max}$ (cm^{-1})	$\Delta\tilde{\nu}_{1/2}$[b] (cm^{-1})
$(pz)(AlR_3)_2$	481 (6900)	20790	7600
$(bp)(AlR_3)_2$	407	24570	8800
$(tmpz)(AlR_3)_2$	350sh (1200)	28570sh	~7000
$(pz)(GaR_3)_2$	427 (3000)	23420	8800
$(bp)(GaR_3)_2$	365	27400	8400
$(pz)(ZnR_2)_2$	370sh (<1000)	27000sh	~7000
$(tmpz)(ZnR_2)_2$	345sh (<1000)	28990sh	~6500

[a]n-Pentane or n-heptane.
[b]Bandwidth at half height.

indicating an acceptor ligand-based LUMO and a HOMO made up of metal-to-carbon bonds (σ bond combination [6]). Most characteristically, the lower LUMO level of the pz relative to the bp complex also shows up as a bathochromically shifted LLCT band, the difference of 3780 cm^{-1} = 0.47 eV corresponding to the 0.31 V difference in the reduction potentials. Considering a large reorganization energy between the relaxed and the non-relaxed LLCT excited state, this correspondence of electrochemical and optical absorption data is quite satisfactory. The large geometrical changes typical for most charge transfer transitions are also reflected by the broadness of these bands (see Fig. 2) with typical band widths at half height of about 8000 cm^{-1} (Table 4). Characteristically, the differences ΔE_{pa} (in V) of electrochemical peak potentials for oxidation and reduction (Table 3) correspond to the energies at the long-wavelength onsets of the LLCT bands: 770 nm ≙ 13 000 cm^{-1} = 1.61 eV (pz complex [20]) and 680 nm ≙ 14 700 cm^{-1} = 1.82 eV (bp complex). Compared to the energies at the absorption maxima, the ΔE_{pa} values show differences of about 1 (e)V, in agreement with the broadness of the LLCT bands and large reorganization energies.

Nevertheless, the complex $(pz)(Al^iPr_3)_2$ shows an unusually large value of 6900 M^{-1} cm^{-1} for the molar extinction coefficient ϵ, signifying a very much overlap-allowed LLCT process with an oscillator strength $f = 4.60 \times 10^{-9}$ $\epsilon\Delta\nu_{1/2}$ [26] = 0.24. The absorption spectrum of the dissociatively labile tmpz complex exhibits a broad long-wavelength band with a maximum at about 350 nm (ϵ 1200 M^{-1} cm^{-1}), suggesting a higher lying π^* MO and a weakened metal–ligand interaction; both effects are expected results from the substitution with sterically demanding and electron-donating methyl groups.

2.1.1.5. ESR spectroscopy

There is no evidence from NMR line broadening or ESR spectroscopy for radical formation and single electron transfer reactivity of the dinuclear complexes at room temperature and in the absence of light. When not sufficiently purified organoaluminium reactants were used there was formation of small amounts of ill-defined (unsymmetrical) radicals [20] with ESR signals indicating the coupling with ^{27}Al nuclei (I = 5/2, 100% natural abundance). Most likely, hydridic impurities are responsible for this apparent electron transfer reactivity; the small, easily bridging hydride ligands lower the kinetic barrier for inner-sphere SET reactivity [1] as has been shown previously in reactions of N-heterocycles with AlH_3 [27] or iso-Bu_2AlH [28]. Irradiation of toluene solutions of $(pz)(Al^iPr_3)_2$ with a mercury lamp in the cavity of an ESR spectrometer did not produce any ESR signals [6] either, however, a bleaching of the intensely purple solutions was observed.

2.1.1.6. LLCT photochemistry

The photoreactivity of $(pz)(Al^iPr_3)_2$ was first studied with regard to wavelength dependence in a cuvette for absorption spectroscopy. A cooled 3.5×10^{-4} M solution in n-hexane was irradiated with a high-pressure mercury lamp equipped with a 400 nm cut-off filter and changes in absorption spectra were followed with time (Fig. 1). While the LLCT band disappeared there were no isosbestic points, the almost colorless solution of the final products exhibited a long-wavelength absorption at about 340 nm. Variation of filters showed that there was slow bleaching within hours even on irradiation with wavelengths of 550 nm or higher, however, efficient bleaching occurred only when the major part of the LLCT absorption was exposed to photons.

Preparative photolysis in a falling-film photoreactor was carried out with 0.01–0.06 M solutions of $(pz)(Al^iPr_3)_2$ at ambient temperatures (in n-hexane) or at 0 °C (in n-pentane), using a high-pressure mercury lamp. After irradiating the dark red solution for several hours, the yellow solution was collected, the solvent removed and the brownish oily product studied by NMR in C_6D_6. Many intense signals between 0.2 and 1.8 ppm and some weak resonances up to 3.5 ppm were observed in the ^{1}H NMR spectrum, however, there were no resonances indicating aromatic or olefinic functions.

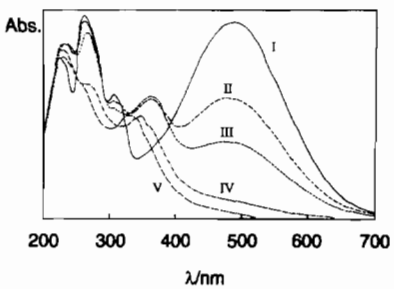

Fig. 1. Changes in the absorption spectrum of a 3.5×10^{-4} M solution of $(pz)(Al^iPr_3)_2$ in n-hexane on irradiation with a high-pressure mercury lamp equipped with a 400 nm filter. Initial solution (I) and spectra after 14 (II), 21 (III), 35 (IV) and 45 (V) min.

Corresponding results were obtained from ^{13}C NMR spectroscopy. After hydrolysis and separation from aluminium hydroxide, a similar result was found for the yellowish oil obtained, suggesting a mixture of saturated compounds. In situ irradiation of a cooled NMR tube containing a 0.25 M solution of $(pz)(Al^iPr_3)_2$ in C_6D_6 solution showed a decrease of the pyrazine resonance while there was no sign for a partially reduced heterocycle which should be expected to have signals higher than 4.6 ppm [29,30]. A large number of intense resonances between 0.3 and 1.7 ppm and a few weak signal groups between 2.0 and 4.3 ppm suggest the presence of several different saturated reaction products.

Summarizing, the complex $(pz)(Al^iPr_3)_2$ is photoreactive upon irradiation into the LLCT band, however, the absence of detectable radical intermediates, isosbestic points and unsaturated products indicates a more complicated photoreaction than the one observed for the system $(DAB)ZnR_2$, DAB = 1,4-disubstituted 1,4-diazabutadiene [6]. The reasons for such complications lie in the dinuclear character of the complex with six metal-to-carbon bonds, in the non-chelate situation and in the well known instability of partially reduced pyrazines [29,30]; the $(DAB)ZnR_2$ systems, on the other hand, have a much lower number of degrees of freedom due to their rigid mononuclear chelate structure with only two fixed metal-to-carbon bonds [6].

2.1.2. Complexes $(\mu\text{-}L)(Ga^iPr_3)_2$

2.1.2.1. Synthesis and stability

The dark red compound $(pz)(Ga^iPr_3)_2$ and the orange complex $(bp)(Ga^iPr_3)_2$ were obtained as very sensitive and labile compounds. Attempts to prepare $(tmpz)(Ga^iPr_3)_2$ failed, no color effect was visible after mixing the components. This difference to the very labile but still isolable aluminium analogue is a consequence of the lower Lewis acidity of GaR_3 compared to AlR_3 while the steric requirements, e.g. the M–C bond lengths, are comparable [31].

2.1.2.2. NMR and ESR spectroscopy

The dinuclear triorganogallium complexes show similar ^1H and ^{13}C NMR effects of coordination as the aluminum analogues (Tables 1 and 2). Line broadening or ESR signals from radicals produced via electron transfer could not be observed.

2.1.2.3. Electrochemistry

Cyclic voltammetry of $(pz)(Ga^iPr_3)_2$ in dichloromethane showed irreversible oxidation at slightly lower potentials than for the Al analogue (Table 3). The reversible reduction is facilitated relative to that of free pyrazine [30] but requires a distinctly more negative potential than that of $(pz)(Al^iPr_3)_2$. This result reflects quantitatively the much diminished Lewis acidity of GaR_3 in relation to AlR_3.

2.1.2.4. Absorption spectroscopy

The absorption spectra of the complexes in pentane show intense, broad LLCT bands (Fig. 2, Table 4). The dissociative tendency of the complex $(pz)(Ga^iPr_3)_2$ is evident from a slight hypsochromic shift of the LLCT band upon dilution due to formation of the mononuclear complex, therefore, rather concentrated solutions had to be studied in 1 mm cuvettes. The difference of 3980 cm^{-1} between the LLCT absorption maxima of the pz complex and the dissociatively less labile bp compound is similar to the one observed for the aluminium analogues. According to the electrochemical results, the generally higher transition energies of the gallium complexes are due to a less stabilized π^* LUMO and thus to the lower polarizing capability of GaR_3 relative to AlR_3. The difference in energies at the absorption maxima of the two pz complexes (2630 $cm^{-1} = 0.33$ eV) corresponds to the electrochemical difference of 0.42 V between the values ΔE_{pa} (Table 3) of the two complexes. Reorganization energies are thus comparable as suggested by the similar bandwidths of the LLCT absorptions (Table 4). As for the aluminium analogues, the energy at the long-wavelength onset of the band at about 640 nm (1.94 eV) agrees with the ΔE_{pa} value of 1.92 V as determined electrochemically (Table 3).

The lower intensity of the LLCT band in the case of the gallium complex relative to the Al analogue (Table 4) is probably due to less effective overlap between $\pi^*(pz)$ and the more diffuse $\sigma(Ga–C)$ bond orbitals.

2.1.2.5. ESR spectroscopy, LLCT photochemistry

Like the aluminium analogues, the gallium complexes were photoreactive without showing ESR detectable radical intermediates or products. Irradiation of a C_6D_6 solution of $(pz)(Ga^iPr_3)_2$ (0.25 M) in a cooled NMR tube gave the same results as in the case of the Al complex, i.e. bleaching and the formation of many intense signals from aliphatic groups between 0.4 and 1.8 ppm. Only very weak resonances were observed between 2.5 and 5.2 ppm, the amount of potentially

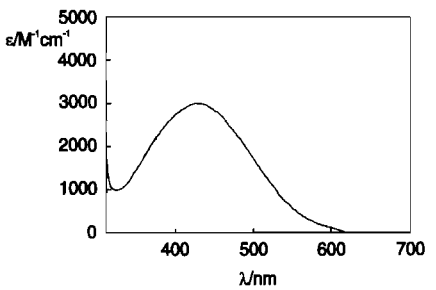

Fig. 2. Absorption spectrum of $(pz)(Ga^iPr_3)_2$ in n-pentane (0.045 M, 1 mm cuvette).

unsaturated intermediates being very small. Apparently, the reactivity of primary group transfer intermediates with partially reduced pyrazine is so high as to allow rapid follow-up reactions which eventually yield saturated systems.

2.1.3. Complexes (μ-L)(Zn^iPr_2)$_2$

2.1.3.1. Synthesis and stability

The orange–yellow solution obtained after mixing the components produced extremely sensitive red crystals of the dinuclear adduct (pz)(Zn^iPr_2)$_2$ which disintegrated slowly even at low temperatures. Lability towards intramolecular electron transfer (see below) and dissociation are most probably due to the comparatively poor Lewis acidity of ZnR_2 and to the low coordination number at the metal. On the other hand, the yellow–orange compound (tmpz)(Zn^iPr_2)$_2$ proved to be less labile than the pz analogue, this different stability order in comparison to the MR_3 complexes possibly being a result of steric protection of coordinatively unsaturated Zn by the methyl substituents. This argument implies a conformation in which the C–Zn–C planes and the π plane of the heterocycle do not coincide, an argument which is supported by the thermochromism of the compound (see below). Attempts to synthesize (bp)(Zn^iPr_2)$_2$ from the components yielded a red–brown precipitate which was not sufficiently soluble in non-coordinating solvents and could thus not be studied further; again, the coordinative unsaturation at Zn is held responsible for this behavior.

2.1.3.2. NMR spectroscopy

The above mentioned difference between the rather stable tmpz complex and the very labile bis-adduct (pz)(Zn^iPr_2)$_2$ is also evident from NMR spectroscopy. Whereas the former complex can be conveniently studied in C_6D_6 solution, the latter compound disintegrates slowly under formation of an NMR (line-broadening) and ESR detectable radical complex, eventually yielding elemental zinc. ^{1}H NMR line-broadening is strongest for the pyrazine protons, suggesting a heterocycle-based radical (see below). The NMR shifts (Tables 1 and 2) are comparable to those of the AlR_3 and GaR_3 complexes but less pronounced, reflecting the lower Lewis acidity of ZnR_2.

2.1.3.3. ESR spectroscopy

The complex (pz)(Zn^iPr_2)$_2$ spontaneously forms radicals in solution in what is believed to be an intramolecular electron transfer process. The best resolved ESR signals were obtained when pyrazine and 2 equiv. of Zn^iPr_2 were reacted in THF solution (Fig. 3). The spectrum clearly shows the occupation of the pyrazine π^* orbital by one electron [30]. Comparison with related species (Table 5) [3,32] suggests the presence of a bis(organozinc) complex of pyrazine radical anion, the

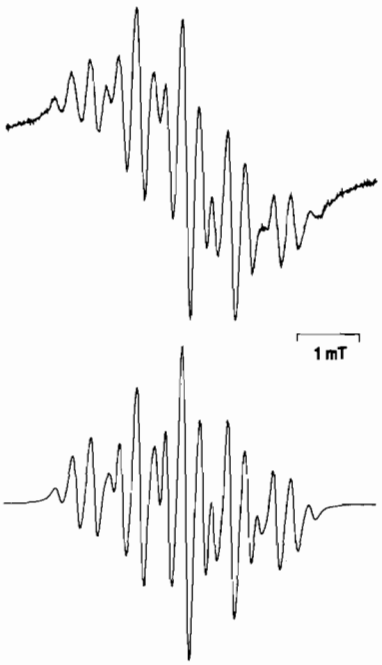

Fig. 3. ESR spectrum of the radical complex obtained after adding pyrazine and Zn^iPr_2 in THF: experimental spectrum (top) and computer simulation (bottom) with the data from Table 5 and 0.13 mT linewidth.

Table 5
ESR data of radical complexes $[(MR_m)(pz)(MR_n)]^{\bullet -}$ [a]

	$a(^{14}N)$	$a(^1H$, pz)	Reference
$[(pz)(Zn^iPr_2)_2]^{\bullet -}$ or $[(^iPr_2Zn)(pz)(Zn^iPr)]^{\bullet}$ [b]	0.745	0.286	this work
$[(pz)(ZnPh_2)_2]^{\bullet -}$ [c]	0.763	0.283	[32] [d]
$[(Ph_2Mg)(pz)(MgPh)]^{\bullet}$	0.680	0.360 0.310	[3,32] [e]
$[(pz)(MgPh_2)_2]^{\bullet -}$	0.677	0.285	[3,32] [d]

[a] Coupling constants a in mT.
[b] ^{67}Zn coupling not observed.
[c] $a(^{67}Zn) = 0.083$ mT.
[d] Reformulated as anionic complex.
[e] Reformulated as dinuclear complex.

values of non-coordinated $pz^{\bullet -}$ in THF being $a(^{14}N)$ 0.718 mT, $a(^1H)$ 0.264 mT and g 2.0035. Unfortunately, the attainable resolution did not allow us to decide whether an anionic complex $[(\mu\text{-pz})(ZnR_2)_2]^{\bullet -}$ or a neutral species $[(R_2Zn)(\mu\text{-pz})ZnR]^{\bullet}$ is present; the spectral asymmetry of the latter primary complex of a homolysis following intramolecular electron transfer is relatively small as has been shown for magnesium analogues [3]. The established capability of such radical complexes to serve as carbanion carriers permits the formation of anionic radical complexes with solvent-stabilized cations $R_{n-1}M^+$ as counterions [6]. Such cationic species are the result of the common carbanion exchange equilibria (4) in solutions of coordinatively unsaturated main group metal alkyls. Due to the small magnetic moment and a low natural abundance of only

4% a metal isotope coupling with ^{67}Zn ($I=5/2$) could not be detected.

2.1.3.4. Electrochemistry

The dissociative lability of the coordinatively unsaturated diorganozinc complexes precluded cyclic voltammetric studies in the necessarily polar electrolyte solutions.

2.1.3.5. Absorption spectroscopy

The LLCT absorption bands of the complexes with Zn^iPr_2 are less intense ($\epsilon < 1000\ M^{-1}\ cm^{-1}$) than those with Al^iPr_3 or Ga^iPr_3. As a solid, the more stable tmpz complex shows thermochromism, i.e. a light yellow color at −80 °C and a yellow–orange appearance at room temperature. In the yellow n-pentane solution the LLCT band appears as a long-wavelength shoulder of $\pi \rightarrow \pi^*$ transitions in the near UV region. The corresponding pz complex exhibits similar absorption features, only bathochromically shifted (Table 4), in agreement with the lower lying π^* MO of the non-methylated pyrazine ligand. While the generally higher energy absorption of the Zn complexes in comparison to Al and Ga analogues is a consequence of a less stabilized π^* LUMO due to the less Lewis acidic organometallic fragment, the thermochromism and lower intensity of the LLCT bands are probably the result of a more sensitive response towards geometry changes at the coordination sites: a rotation of the C–Zn–C and π planes along the Zn–N axis requires probably little activation energy but strongly affects the overlap between σ(Zn–C) and π^* orbitals. In the (DAB)ZnR_2 complexes, on the other hand, the orientation is fixed due to the rigid chelate situation and the extinction coefficient ϵ of a LLCT absorption band has been determined to be 1200 $M^{-1}\ cm^{-1}$ in one instance [6].

2.2. Complexes with 2,2′-bipyridine (bpy)

2.2.1. Reaction between bpy and Al^iPr_3

Although 2,2′-bipyridine is one of the prototypical chelate ligands in coordination chemistry [33], it is capable of forming non-chelate complexes with electrophiles such as $M(CO)_5$ (M = Cr, W) or AlR_3 (R = Me, Et) [15–17] which offer only one open coordination site. Adducts (η^1-bpy)(AlR_3) and (μ-bpy)(AlR_3)$_2$ were reported with the aluminium alkyls mentioned, however, the complex with $AlEt_3$ was reported to decompose under formation of paramagnetic products [16]. We have now studied the reaction between bpy and the more electron rich Al^iPr_3 in order to define both diamagnetic precursor and radical products. Experiments involving ZnR_2 and non-aromatic α-diimine ligands have demonstrated [6,34] an increasing reactivity of the precursor complexes towards electron transfer and thus radical formation with the electron donating capability of R, i.e. in the sequence Me < Et < ^{i}Pr < tert-Bu.

In fact, the reaction between Al^iPr_3 and bpy at ambient temperature in n-pentane produced immediately a brown solution which displayed a strong and persistent ESR signal. The radical could be identified as the SET escape product [(bpy$^{\cdot-}$)($^+AlR_2$)], R = ^{i}Pr, according to the spectral similarity with other such radicals (R = H, Me, Et, ^{i}Bu [27,28,35,36a]; see Table 7). Oxidative hydrolysis of the red–brown oil obtained after removal of the solvent gave a yellowish solid which contained mainly bpy (^1H, ^{13}C NMR); alkylation of the aromatic heterocycle was not a major reaction under these conditions.

When the reaction was carried out at −60 °C, a diamagnetic yellow adduct (η^1-bpy)Al^iPr_3 precipitated which began to disintegrate above −30 °C. At room temperature the solid decomposed within minutes to a brownish oil. The ^1H and ^{13}C NMR spectra taken at −53 °C in $CDCl_3$ confirm the suggested unsymmetrical η^1-coordination of bpy to Al^iPr_3 (Table 6) by showing signals for two different pyridyl rings; two of the ^1H signals are broadened, presumably due to effects of hindered rotation.

Summarizing, the reaction between bpy and Al^iPr_3 yields an unsymmetrical 1:1 adduct with η^1-coordinated bpy as low temperature-stable precursor complex. The formation of a diamagnetic chelate complex involving η^2-bpy and then pentacoordinate aluminium is not observed, instead, there is facile intra-complex conversion to the radical complex with again tetracoordinate metal (7). This eventual homolysis of a metal-to-carbon bond is supposed to have a strong intramolecular SET component because the resulting radical product contains an electron in the π^*(bpy) acceptor orbital whereas the (bpy$^{\cdot-}$)-coordinated cation $^+AlR_2$ can be viewed

Table 6
NMR data of [(AlR_3)(bpy)], R = ^{i}Pr, at −53 °C and bpy at 25 °C[a]

	δ(^{1}H)		δ(^{13}C)	
	Complex	bpy	Complex	bpy
CH(CH$_3$)$_2$	−0.16		10.5	
CH(*CH*$_3$)$_2$	[b]		21.3	
*C*1			155.5	156.4
			155.9	
*H*3/*C*3	8.2(br)	8.42	149.1	149.4
	7.74		149.5	
*H*4/*C*4	8.0	7.73	124.0[c]	124.0
	7.85		124.4[c]	
*H*5/*C*5	7.57	7.21	137.3	137.2
	7.34		138.5	
*H*6/*C*6	8.70	8.65	121.0	121.4
	8.6(br)		125.7[c]	

[a]In $CDCl_3$, ^1H NMR assignments based on spin–spin coupling patterns.
[b]Not determined due to signal overlapping with traces of pentane.
[c]Tentative assignments.

as a secondary product of the one-electron oxidation of AlR_3, involving reaction (3).

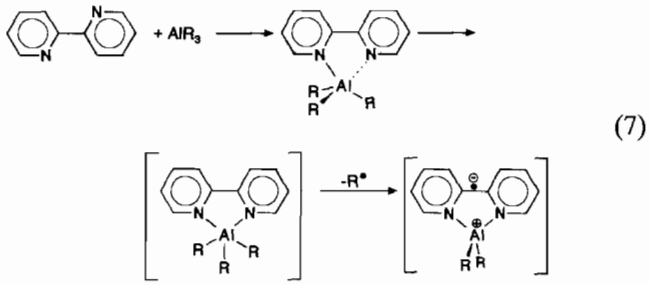

(7)

As in the case of ET-active complexes $(DAB)ZnR_2$ [6], the overlap between electron-rich M–C bonds and the π^* acceptor orbitals in a chelate situation strongly favors the assumed SET-induced homolysis.

2.2.2. Isolation of $(\eta^2\text{-bpy})Al[CH(SiMe_3)_2]_2$

The radical complexes $[(bpy^{\bullet-})(^+AlR_2)]$ formed via single electron transfer [16,27,28] could not be isolated in pure form because cage and escape processes yield a mixture of products. A more controlled way to produce such rather stable species is to react bpy with an alkali metal such as potassium and with the appropriate halide R_2AlX because the only other product, the alkali metal halide, should be conveniently separated in non-polar solvents, the radical complex being neutral and thus well soluble. We have carried out such a reaction in THF using bis(bis(trimethylsilyl)methyl)aluminium chloride because the steric bulk of the resulting complex promised to guarantee better protection of the sensitive bpy radical anion ligand and because the related diamagnetic zinc(II) complex $(\eta^2\text{-bpy})Zn[CH(SiMe_3)_2]_2$ had been structurally characterized [37]. The other side of the assumed and found stability of the paramagnetic complex with bulky substituents is that the trisubstituted aluminium compound $Al[CH(SiMe_3)_2]_3$ does not react at all with bpy, most likely due to its reluctance to pyramidalization at the metal center.

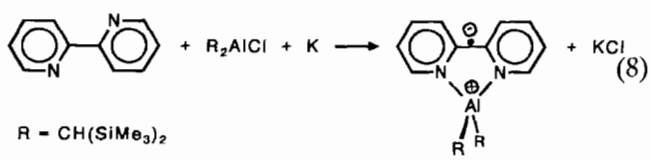

(8)

The dark green air-sensitive solid obtained via the classical route (8) was characterized by mass spectroscopy and elemental analysis as the desired product. The oxidation state distribution $(bpy^{\bullet-})Al^{III}$ instead of $(bpy)Al^{II}$ was confirmed not only by ESR (Table 7) but also via absorption spectroscopy (Fig. 4, Table 8). The radical anion of 2,2′-bipyridine [38,39] and also its complexes [40,41] are distinguished by long-wavelength intraligand absorption bands which are due to transitions involving the singly occupied π^* MO (π_7) and which often display vibrational fine structure in the order of 1000 cm^{-1} (ring vibrations). Such features are also observed for $(bpy)Al[CH(SiMe_3)_2]_2$ (Fig. 4), the shifts of absorption energies relative to those of non-coordinated $bpy^{\bullet-}$ being rather small (Table 8).

The compilation of ESR data for the complexes $[(bpy^{\bullet-})(^+AlR_2)]$ (Table 7) shows significant differences only for the ^{27}Al hyperfine coupling which directly reflects the effects of the substituents R. Both the electron donor capacity of these substituents and their steric requirements, affecting for example the Al–N bond lengths, should play a role in determining $a(^{27}Al)$; the highest coupling constants and thus strongest interactions are found for the dihydride and for the complex with the electron-donating but not yet too bulky isopropyl groups.

The dissociative stability of the radical complex $(bpy)Al[CH(SiMe_3)_2]_2$ allowed us to determine its elec-

Table 7
ESR parameters of radical complexes $[(R_2M)(bpy)]^{\bullet}$[a]

M	R	a_N	a_{H3}	a_{H4}	a_{H5}	a_{H6}	a_M[b]	g	Reference
Al	H	0.29	[c]	0.29	0.29	[c]	0.46	2.0030	[27]
Al	Me	0.304	0.026	0.304	0.259	0.026	0.404	2.0030	[35]
Al	Et	0.300	0.028	0.300	0.270	0.028	0.436	2.0030	[35]
Al	^{i}Pr	0.314	[c]	0.285	0.285	[c]	0.457	2.0028	this work
Al	^{i}Bu	0.304	0.028	0.304	0.263	0.028	0.437	[c]	[28]
Al	R′[d]	0.299	0.027	0.304	0.269	0.027	0.400	2.0030	this work
Ga	CH_3	0.350	[c]	0.350	0.233	0.050	1.185/ 1.505	2.0028	[36]
Ga	^{i}Pr	0.352	[c]	0.350	0.223	0.056	1.332/ 1.692	2.0031	this work

[a]Coupling constants a in mT.
[b]$a(^{27}Al)$ or $a(^{69}Ga/^{71}Ga)$.
[c]Not observed or reported.
[d]$R' = CH(SiMe_3)_2$.

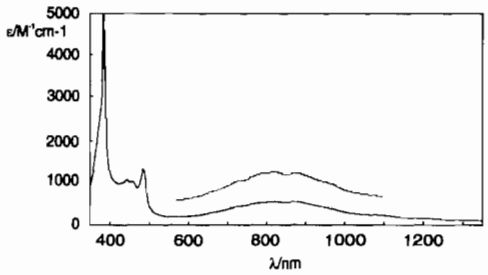

Fig. 4. Absorption spectrum of $(bpy)Al[CH(SiMe_3)_2]_2$ in n-pentane.

Table 8
Absorption maxima λ_{max} (nm) of $[(R_2Al)bpy]^{\bullet}$, $R = CH(SiMe_3)_2$[a], and $bpy^{\bullet-}$[b]

	$\pi_6 \rightarrow \pi_7$[c]	$\pi_7 \rightarrow \pi_{10}$	$\pi_7 \rightarrow \pi_{8/9}$
$[(R_2Al)bpy]^{\bullet}$	375, 384	442, 459, 486	737sh, 819, 878, 950sh
$bpy^{\bullet-}$	385, 393	513, 540, 588	675, 760, 850, 1050

[a]In pentane (295 K).
[b]In 2-methyl-THF (77 K), Ref. [38].
[c]Assignments of transitions; π_7: singly occupied MO, Ref. [39].

trochemical oxidation potential in dichloromethane (Fig. 5). The transition (9) is reversible, the potential of −1.26 V versus ferrocene/ferrocenium corresponding to −0.85 V versus SCE. In relation to other complexes of bpy [12], this value indicates a significantly stronger acceptor effect of $^{+}AlR_2$ than that of, for example, $Zn(tert\text{-}Bu)_2$ or $^{+}Cu(PPh_3)_2$ [12]; only diquaternized bpy compounds such as diquat [42] show still less negative reduction potentials of about −0.6 V versus SCE. This sequence of electrochemically determined acceptor effects parallels the ESR results obtained previously [36a]. The aluminium(III) radical complex is irreversibly oxidized at +0.75 V versus ferrocene.

$$[(bpy^{-})AlR_2]^{\cdot} \rightleftharpoons [(bpy)AlR_2]^{+} + e^{-} \quad (9)$$

2.2.3. Reaction between bpy and Ga^iPr_3

Mixing both components in n-pentane produces briefly a yellow color which rapidly changes to a red paramagnetic solution. Attempts to isolate the red product by crystallization failed due to slow decomposition processes. The intense ESR signal obtained can be well resolved (Fig. 6) and indicates the formation of the SET escape product $[(bpy^{\cdot -})(^{+}GaR_2)]$, R = ^{i}Pr, as evident from the spectral analogy with a related radical (R = Me [36]; Table 7). As in the case of the aluminium complexes, the isopropyl derivative exhibits higher metal coupling constants than the methyl analogue: ^{69}Ga (60%, I = 3/2), ^{71}Ga (40%, I = 3/2), $\mu(^{71}Ga)/\mu(^{69}Ga) = 1.27$. The complex must clearly be formulated as the Ga(III) complex of the bpy radical anion, similarly to complexes $[Ga(DAB)_2]$ [43] which have to be formulated as $(DAB^{2-})Ga^{III}(DAB^{\cdot -})$ [44]. It is assumed that a similar sequence of events (7) occurs here as for the aluminium complexes. In contrast to GaR_3, AlR_3 and MgR_2 [45], Zn^iPr_2 and other diorganozinc complexes react with bpy to yield only colored (LLCT) diamagnetic complexes with four-coordinate metal and no tendency towards electron transfer-induced homolysis [37,46–48]; the formation of anionic radical complexes $[(bpy)(ZnR_2)]^{\cdot -}$ requires external chemical or electrochemical reduction [36].

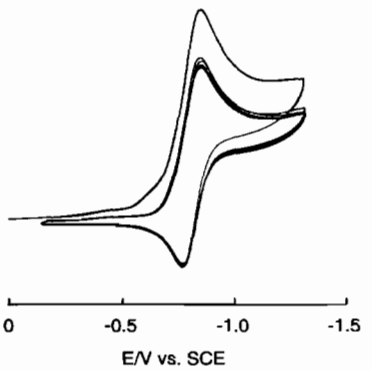

Fig. 5. Cyclic voltammogram of $(bpy)Al[CH(SiMe_3)_2]_2$ in dichloromethane/0.1 M Bu_4NPF_6.

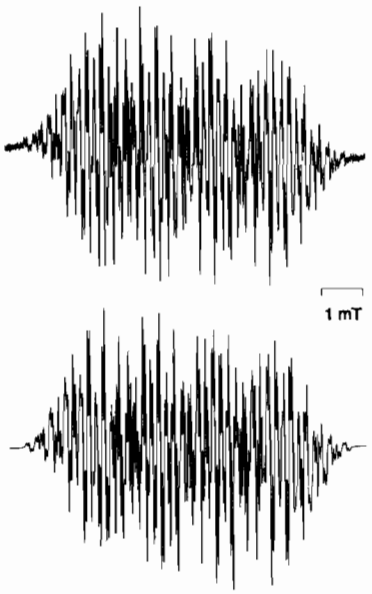

Fig. 6. ESR spectrum of $(bpy)Ga(^iPr)_2$ in n-pentane: experimental spectrum (top) and computer simulation (bottom) with the data from Table 7 and 0.042 mT linewidth.

3. Conclusions

This work was undertaken in order to obtain more information on the known tendency of aluminium and zinc alkyls to form colored intermediates [6,16,17, 20,37,46–51] and paramagnetic products [3,6,28,36,52] with π acceptor substrates. The presented dinuclear organometallic complexes with coordinatively saturated metal centers clearly exhibit interactions between the σ(M–C) orbitals of the organometallic donor components and the π^* orbitals of the bridging acceptor ligands, as evident from NMR and LLCT absorption spectroscopy. Particularly large spectroscopic (λ_{max}, ϵ) and electrochemical effects were observed for the combination between the electron-rich and Lewis acidic Al^iPr_3 molecules and the small π acceptor system pyrazine. Sterically encumbered tetramethylpyrazine and the larger π system 4,4′-bipyridine exhibit smaller effects. Although these adducts can be viewed as precursor complexes of SET reactions, no such thermally induced processes were observed except for the coordinatively least saturated system $(pz)(Zn^iPr_2)_2$. Irradiation into the LLCT band of pz complexes resulted in photoreactivity, however, simple group transfer intermediates could not be observed due to the apparent reactivity of partially reduced heteroaromatics and a cascade reaction leading to mainly saturated products.

Using the bpy chelate system, thermal radical-producing reactions were observed with Al^iPr_3 and Ga^iPr_3

which apparently result from a strong tendency towards the optimal coordination number four. A particularly stable radical complex, (bpy)Al[CH(SiMe$_3$)$_2$]$_2$, could now be isolated and characterized beyond ESR spectroscopy. In comparison to the well-behaved and well-documented (DAB)ZnR$_2$ system [6], the Ga and Al species described here are distinguished by a pronounced preference for the coordination number four; the heteroaromatic acceptors (4), on the other hand, suffer from the lability of partially reduced intermediates which results in less defined recombination products in what is assumed to be electron transfer-involving photochemistry. It is apparent from these results how coordinative requirements [24] influence stabilities of precursor complexes and radical products and, thus, the course of electron transfer reactions.

4. Experimental

4.1. Instrumentation

NMR spectrometers: Bruker AM 200 and AC 250. ESR spectrometer: Bruker ESP 300 (X band); *g* factor determination with a Bruker NMR gaussmeter ER 035 M and a microwave counter HP5350B. UV–Vis–NIR absorption spectrophotometer: Shimadzu UV160 and Bruins Instruments Omega 10. Mass spectrometer: Varian MAT 711. Elemental analysis: Mikroanalytisches Labor Pascher, Remagen, Germany. Cyclic voltammetry: Potentiostat EG&G model 363, function generator EG&G 175, glassy carbon working electrode, Pt counter electrode, Ag/AgCl or SCE as reference (internal standard: ferrocene/ferrocenium couple). Photochemistry: Falling film photoreactor N 9356 (Normag, Hofheim, Germany), high-pressure mercury lamps TQ 50 and Q 180 (Heraeus, Hanau, Germany) and HBO 50W/AC (Spindler & Hoyer, Göttingen, Germany); cut-off filters from Schott (Mainz, Germany).

4.2. Syntheses

All synthetic manipulations and physical measurements had to be carried out under an argon atmosphere, using dried solvents. Diisopropylzinc and triisopropylgallium were obtained according to literature procedures [53,54]; triisopropylaluminium and bis(bis(trimethylsilyl)methyl)aluminium chloride were supplied by Dr A. Vester and Professor W. Uhl, Oldenburg [55]. Reliable elemental analyses of the dinuclear adducts could not be obtained due to their dissociative lability; identity and purity of the isolated materials were established by NMR as summarized in Tables 1 and 2.

4.2.1. (pz)(Al^{i}Pr$_3$)$_2$

Mixing of 0.16 g (2.0 mmol) pyrazine and 0.624 g (4.0 mmol) triisopropylaluminium in 20 ml pentane produces a deep purple solution. About 0.6 g (75%) of very air-sensitive dark red crystals were obtained after cooling to −30 °C.

Attempts to prepare (pz){Al[CH(SiMe$_3$)$_2$]$_3$}$_2$ by reacting the components in the appropriate ratio for several hours in n-pentane did not produce any color; precipitation brought on by cooling to −80 °C yielded only unreacted colorless Al[CH(SiMe$_3$)$_2$]$_3$.

4.2.2. (tmpz)(Al^{i}Pr$_3$)$_2$

To a solution of 0.272 g (2.0 mmol) tetramethylpyrazine in 10 ml pentane was added 0.624 g (4.0 mmol) of triisopropylaluminium. The red solution was cooled to −10 °C upon which ~0.6 g (65%) of very air-sensitive red crystals were collected which slowly disintegrated at ambient temperatures.

4.2.3. (bp)(Al^{i}Pr$_3$)$_2$

Addition of 0.312 g (2.0 mmol) triisopropylaluminium to 0.156 g (1.0 mmol) 4,4′-bipyridine in 20 ml pentane produced an orange precipitate. After 2 h stirring at ambient temperatures about 0.4 g (85%) of very air-sensitive orange material was collected by filtration.

4.2.4. (pz)(Ga^{i}Pr$_3$)$_2$

Mixing of 0.16 g (2.0 mmol) pyrazine and 0.80 g (4.0 mmol) triisopropylgallium in 15 ml pentane immediately produced a deep red solution. About 0.6 g (60%) of very air-sensitive dark red crystals were obtained after cooling to −30 °C.

4.2.5. (bp)(Ga^{i}Pr$_3$)$_2$

Addition of 0.40 g (2.0 mmol) triisopropylgallium to 0.156 g (1.0 mmol) 4,4′-bipyridine in 25 ml pentane produced an orange precipitate. After 2 h stirring at ambient temperatures about 0.45 g (80%) of very air-sensitive orange material was collected by filtration.

4.2.6. (pz)(Zn^{i}Pr$_2$)$_2$

Mixing of 0.08 g (1.0 mmol) pyrazine and 0.302 g (2.0 mmol) diisopropylzinc in 15 ml pentane produced an orange–yellow solution. After cooling to −30 °C a few red crystals had precipitated which were collected by removal of the solvent and by drying under high vacuum at −60 °C. About 0.2 g (50%) of very sensitive dark red crystals was thus obtained.

4.2.7. (tmpz)(Zn^{i}Pr$_2$)$_2$

To a solution of 0.204 g (1.5 mmol) tetramethylpyrazine in 10 ml pentane was added 0.454 g (3.0 mmol) of diisopropylzinc. The yellow solution was cooled to −30 °C upon which about 0.3 g (45%) of very air-sensitive yellow–orange crystals was collected.

4.2.8. (bp)(Zn^iPr_2)$_2$

Addition of 0.485 g (3.2 mmol) diisopropylzinc to a solution of 0.25 g (1.6 mmol) 4,4′-bipyridine produced a red–brown precipitate which was filtered off, washed with n-pentane and dried under vacuum. The solid was insoluble in aliphatic, aromatic and chlorinated hydrocarbons and showed signs of slow decomposition at ambient temperatures.

4.2.9. (η^1-bpy)Al^iPr_3

A solution of 0.312 g (0.2 mmol) 2,2′-bipyridine in 50 ml n-pentane was cooled to −60 °C and 0.312 g (0.2 mmol) triisopropylaluminium was slowly added. A yellow precipitate formed immediately and the mixture was stirred for 2 h before the solvent was removed by decanting. The remaining solid was then vacuum-dried at −60 °C and used for NMR spectroscopy. At temperatures above −30 °C the solid began to decompose, visible by browning.

4.2.10. (η^2-bpy)Al[CH($SiMe_3$)$_2$]$_2$

A solution of 0.57 g (1.5 mmol) bis(bis-(trimethylsilyl)methyl)aluminium chloride and 0.234 g (1.5 mmol) 2,2′-bipyridine were dissolved in 50 ml THF and then treated with 0.06 g (1.5 mmol) potassium metal. After stirring for 1 day the dark green solution was filtered to remove most of the KCl. Removal of THF, addition of 50 ml toluene and another filtration gave a solution which was reduced to about 10 ml and cooled to −10 °C to yield a dark green microcrystalline solid (0.706 g, 94%); m.p. 45–47 °C; *m/e* 501.2 (4.2%). *Anal.* Found: C, 55.30; H, 9.12; N, 5.56; Si, 22.4. Calc. for $C_{24}H_{46}AlN_2Si_4$: C, 57.43; H, 9.24; N, 5.58; Si, 22.38%.

Acknowledgements

Support for research on electron transfer phenomena from the Land Baden-Württemberg (Forschungsschwerpunktprogramm), the Volkswagenstiftung (Program: Organometallics in Organic Synthesis), the Deutsche Forschungsgemeinschaft and the Fonds der Chemischen Industrie is gratefully acknowledged. We also thank Dr Annegret Vester and Professor Dr W. Uhl (Oldenburg) for a gift of triisopropylaluminium and bis(bis(trimethylsilyl)methyl)aluminium chloride.

References

[1] W. Kaim, *Top. Curr. Chem., 169* (1994) 231.
[2] J.K. Kochi, *Organometallic Mechanisms and Catalysis,* Academic Press, New York, 1978; *Angew. Chem., 100* (1988) 1331; *Angew. Chem., Int. Ed. Engl., 27* (1988) 1227.
[3] W. Kaim, *Acc. Chem. Res., 18* (1985) 160.
[4] C. Elschenbroich and A. Salzer, *Organometallics. A Concise Introduction,* VCH, Weinheim, Germany, 2nd edn., 1991.
[5] G. Wilkinson, F.G.A. Stone and E.W. Abel (eds.), *Comprehensive Organometallic Chemistry,* Pergamon, Oxford, UK, 1982.
[6] M. Kaupp, H. Stoll, H. Preuss, W. Kaim, T. Stahl, G. van Koten, E. Wissing, W.J.J. Smeets and A.L. Spek, *J. Am. Chem. Soc., 113* (1991) 5606.
[7] J.P. Collman, L.S. Hegedus, J.R. Norton and R.G. Finke, *Principles and Applications of Organotransition Metal Chemistry,* University Science Books, Mill Valley, CA, 1987.
[8] *Prog. Inorg. Chem., 30* (1983) 1–498.
[9] D.G. Tuck, *Coord. Chem. Rev., 112* (1992) 215.
[10] L. Eberson, *Electron Transfer Reactions in Organic Chemistry,* Springer, Berlin, 1987.
[11] (a) A. Pross, *Acc. Chem. Res., 18* (1985) 212; (b) J.K. Cho and S. Shaik, *J. Am. Chem. Soc., 113* (1991) 9890.
[12] W. Bruns, W. Kaim, M. Ladwig, B. Olbrich-Deussner, T. Roth and B. Schwederski, in A.J.L. Pombeiro and J. McCleverty (eds.), *Molecular Electrochemistry of Inorganic, Bioinorganic and Organometallic Compounds,* Kluwer, Dordrecht, Netherlands, 1993, p. 255.
[13] J.-M. Saveant, *Acc. Chem. Res., 26* (1993) 455.
[14] (a) A. Vogler and H. Kunkely, *Top. Curr. Chem., 158* (1990) 1; (b) H. Kunkely and A. Vogler, *J. Organomet. Chem., 453* (1993) 269.
[15] (a) M.J. Schadt, N.J. Gresalfi and A.J. Lees, *J. Chem. Soc., Chem. Commun.,* (1984) 506; (b) S. Cao, K.B. Reddy, E.M. Eyring and R. van Eldik, *Organometallics, 13* (1994) 91.
[16] H. Lehmkuhl and H.D. Kobs, *Liebigs Ann. Chem., 719* (1968) 11.
[17] (a) K.H. Thiele and W. Brüser, *Z. Anorg. Allg. Chem., 348* (1966) 179; (b) *349* (1967) 33.
[18] (a) H. Bock and W. Kaim, *Chem. Ber., 111* (1978) 3552; (b) *Acc. Chem. Res., 15* (1982) 9.
[19] W. Uhl, A. Vester, W. Kaim and J. Poppe, *J. Organomet. Chem., 454* (1993) 9.
[20] J. Baumgarten, C. Bessenbacher, W. Kaim and T. Stahl, *J. Am. Chem. Soc., 111* (1989) 2126 and 5017.
[21] (a) A.S. Chia and R.F. Trimble, *J. Phys. Chem., 65* (1961) 863; (b) P. Krumholz, *J. Am. Chem. Soc., 73* (1951) 3487.
[22] H.D. Hausen, O. Mundt and W. Kaim, *J. Organomet. Chem., 296* (1985) 321.
[23] (a) W. Kaim, *Angew. Chem., 92* (1980) 940; *Angew. Chem., Int. Ed. Engl., 19* (1980) 911. (b) *J. Organomet. Chem., 241* (1983) 157.
[24] W. Kaim, in A. Müller, E. Diemann, W. Junge and H. Ratajczak (eds.), *Electron and Proton Transfer in Chemistry and Biology,* Elsevier, Amsterdam, 1992, p. 45.
[25] A. Schulz and W. Kaim, *Chem. Ber., 122* (1989) 1863.
[26] D.E. Richardson and H. Taube, *J. Am. Chem. Soc., 105* (1983) 40.
[27] W. Kaim, *J. Am. Chem. Soc., 106* (1984) 1712.
[28] W. Kaim, *Z. Naturforsch., Teil B, 37* (1982) 783.
[29] W. Kaim, *Angew. Chem., 93* (1981) 620; *Angew. Chem., Int. Ed. Engl., 20* (1981) 599.
[30] W. Kaim, *Angew. Chem., 95* (1983) 201; *Angew. Chem., Int. Ed. Engl., 22* (1983) 171.
[31] Organogallium Compounds, Part 1, in *Gmelin Handbook of Inorganic Chemistry,* Springer, Berlin, 1987.
[32] W. Kaim, *Z. Naturforsch., Teil B, 36* (1981) 1110.
[33] W.R. McWhinnie and J.D. Miller, *Adv. Inorg. Chem. Radiochem., 12* (1969) 135.
[34] (a) G. van Koten, in A. de Meijere and H. tom Dieck (eds.), *Organometallics in Organic Synthesis,* Springer, Berlin, 1988, p. 277; (b) G. van Koten, J.T.B.H. Jastrzebski and K. Vrieze, *J. Organomet. Chem., 250* (1983) 49; (c) J.M. Klerks, J.T.B.H. Jastrzebski, G. van Koten and K. Vrieze, *J. Organomet. Chem.,*

224 (1982) 107; (d) J.M. Klerks, D.J. Stufkens, G. van Koten and K. Vrieze, *J. Organomet. Chem., 181* (1979) 271.
[35] W. Kaim, *J. Organomet. Chem., 215* (1981) 325.
[36] (a) W. Kaim, *Chem. Ber., 114* (1981) 3789; (b) M.F. El-Shazly, *Inorg. Chim. Acta, 26* (1978) 173.
[37] M. Westerhausen, B. Rademacher and W. Schwarz, *J. Organomet. Chem., 427* (1992) 275.
[38] T. Shida, *Electronic Absorption Spectra of Radical Ions,* Elsevier, Amsterdam, 1988, p. 197.
[39] (a) E. König and S. Kremer, *Chem. Phys. Lett., 5* (1970) 87; (b) P.S. Braterman and J.-I. Song, *J. Org. Chem., 56* (1991) 4678.
[40] (a) P.S. Braterman, J.-I. Song, C. Vogler and W. Kaim, *Inorg. Chem., 31* (1992) 222; (b) P.S. Braterman, J.-I. Song, F.M. Wimmer, S. Wimmer, W. Kaim, A. Klein and R.D. Peacock, *Inorg. Chem., 31* (1992) 5084.
[41] M. Ladwig and W. Kaim, *J. Organomet. Chem., 439* (1992) 79.
[42] S. Hünig, J. Gross and W. Schenk, *Liebigs Ann. Chem.,* (1973) 324.
[43] (a) F.G.N. Cloke, G.R. Hanson, M.J. Henderson, P.B. Hitchcock and C.L. Raston, *J. Chem. Soc., Chem. Commun.,* (1980) 1002; (b) M.J. Henderson, C.H.L. Kennard, C.L. Raston and G. Smith, *J. Chem. Soc., Chem. Commun.,* (1990) 1203; (c) F.G.N. Cloke, C.I. Dalby, M.J. Henderson, P.B. Hitchcock, C.H.L. Kennard, R.N. Lamb and C.L. Raston, *J. Chem. Soc., Chem. Commun.,* (1990) 1394.
[44] W. Kaim and W. Matheis, *J. Chem. Soc., Chem. Commun.,* (1991) 597.
[45] W. Kaim, *J. Am. Chem. Soc., 104* (1982) 3833, 7385.
[46] G.E. Coates and S.T.E. Green, *J. Chem. Soc.,* (1962) 334.
[47] (a) J.G. Noltes and J.W.G. van den Hurk, *J. Organomet. Chem., 3* (1965) 222; (b) J.G. Noltes and J. Boersma, *J. Organomet. Chem., 9* (1967) 1.
[48] T. Stahl, *Ph.D. Thesis,* University of Stuttgart, Germany, 1992.
[49] G. Wittig and O. Bub, *Liebigs Ann. Chem., 566* (1950) 113.
[50] T. Mole, *Aust. J. Chem., 16* (1963) 807.
[51] E.C. Ashby, J. Laemmle and H.M. Neumann, *J. Am. Chem. Soc., 90* (1968) 5179.
[52] G.A. Razuvaev, G.A. Abakumov, E.S. Klimov, E.N. Gladyshev and P.Y. Bayushkin, *Izv. Akad. Nauk SSSR, Ser. Khim.,* (1977) 1128.
[53] G. Hoffmann and R. Fischer, *Z. Anorg. Allg. Chem., 590* (1980) 181.
[54] M.H. Abraham, *J. Chem. Soc.,* (1960) 4130.
[55] W. Uhl, *Z. Naturforsch., Teil B, 43* (1988) 1113.